International Journal of Thermophysics, Vol. 27, No. 5, September 2006 (© 2006)
DOI: 10.1007/s10765-006-0112-8

An Extended Equation of State Modeling Method II. Mixtures

G. Scalabrin,[1] P. Marchi,[1] P. Stringari,[1] and D. Richon[2,3]

Received January 30, 2006

This work is the extension of previous work dedicated to pure fluids. The same method is extended to the representation of thermodynamic properties of a mixture through a fundamental equation of state in terms of the Helmholtz energy. The proposed technique exploits the extended corresponding-states concept of distorting the independent variables of a dedicated equation of state for a reference fluid using suitable scale factor functions to adapt the equation to experimental data of a target system. An existing equation of state for the target mixture is used instead of an equation for the reference fluid, completely avoiding the need for a reference fluid. In particular, a Soave–Redlich–Kwong cubic equation with van der Waals mixing rules is chosen. The scale factors, which are functions of temperature, density, and mole fraction of the target mixture, are expressed in the form of a multilayer feedforward neural network, whose coefficients are regressed by minimizing a suitable objective function involving different kinds of mixture thermodynamic data. As a preliminary test, the model is applied to five binary and two ternary haloalkane mixtures, using data generated from existing dedicated equations of state for the selected mixtures. The results show that the method is robust and straightforward for the effective development of a mixture-specific equation of state directly from experimental data.

KEY WORDS: cubic equation of state; extended equation of state; feed forward neural networks; fundamental equation of state; Helmholtz energy equation; mixtures; thermodynamic properties.

[1] Dipartimento di Fisica Tecnica, Università di Padova, via Venezia 1, I-35131 Padova, Italy.
[2] Centre Energétique et Procédés, Ecole Nationale Supérieure des Mines de Paris CEP/TEP, 35 rue Saint Honoré, 77305 Fontainebleau, France.
[3] To whom correspondence should be addressed. E-mail: dominique.richon@ensmp.fr

1. INTRODUCTION

The development of models for the accurate representation of thermodynamic properties of fluid mixtures is an important task for thermodynamics, since such properties are fundamental input for the design, optimization, and control of processes. Examples for relevant technical applications are the fields of refrigeration and air conditioning, but the interest for such models is much wider and, for instance, comprises many unit operations in chemical engineering.

Mixture models in terms of the Helmholtz energy A play an important role. In fact, they are *fundamental* equations of state (EoS), i.e., all the thermodynamic properties of the system can be calculated from them simply by combinations of derivatives and no integral calculation is required. For a mixture m containing C components, a fundamental EoS can be expressed as

$$\begin{aligned} a_{\mathrm{m}}(T_{\mathrm{m}}, \rho_{\mathrm{m}}, \bar{z}) &= \frac{A^{\mathrm{o}}_{\mathrm{m}}(T_{\mathrm{m}}, \rho_{\mathrm{m}}, \bar{z})}{RT_{\mathrm{m}}} + \frac{A^{\mathrm{R}}_{\mathrm{m}}(T_{\mathrm{m}}, \rho_{\mathrm{m}}, \bar{z})}{RT_{\mathrm{m}}} \\ &= a^{\mathrm{o}}_{\mathrm{m}}(T_{\mathrm{m}}, \rho_{\mathrm{m}}, \bar{z}) + a^{\mathrm{R}}_{\mathrm{m}}(T_{\mathrm{m}}, \rho_{\mathrm{m}}, \bar{z}) \end{aligned} \tag{1}$$

where the reduced Helmholtz energy a_{m} is a function of temperature T_{m}, molar density ρ_{m}, and mole fraction array $\bar{z}$, while R is the universal gas constant.

The ideal part $a^{\mathrm{o}}_{\mathrm{m}}$ reads

$$a^{\mathrm{o}}_{\mathrm{m}}(T_{\mathrm{m}}, \rho_{\mathrm{m}}, \bar{z}) = \sum_{i=1}^{C} z_i a^{\mathrm{o}}_i(T_{\mathrm{m}}, \rho_{\mathrm{m}}) + \sum_{i=1}^{C} z_i \ln(z_i) \tag{2}$$

On the right side of Eq. (2), the first part is a linear combination of the reduced ideal-gas Helmholtz energy a^{o}_i of each of the C components and the second part represents the reduced Helmholtz energy of ideal mixing. The functions $a^{\mathrm{o}}_i(T, \rho)$ are evaluated for each component at the mixture conditions ($T = T_{\mathrm{m}},\ \rho = \rho_{\mathrm{m}}$) from

$$\begin{aligned} a^{\mathrm{o}}_i(T, \rho) = \frac{A^{\mathrm{o}}_i(T, \rho)}{RT} &= \frac{H^{\mathrm{o}}_{i,\mathrm{o}}}{RT} - \frac{S^{\mathrm{o}}_{i,\mathrm{o}}}{R} - 1 + \frac{1}{RT}\int_{T_{\mathrm{o}}}^{T} C^{\mathrm{o}}_{p,i}(T)\, dT \\ &\quad - \frac{1}{R}\int_{T_{\mathrm{o}}}^{T} \frac{C^{\mathrm{o}}_{p,i}(T)}{T}\, dT + \ln\left(\frac{T\rho}{T_{\mathrm{o}}\rho_{\mathrm{o}}}\right) \end{aligned} \tag{3}$$

where only the ideal-gas isobaric heat capacities $C^{\mathrm{o}}_{p,i}(T)$ of the components are required; $H^{\mathrm{o}}_{i,\mathrm{o}}$ and $S^{\mathrm{o}}_{i,\mathrm{o}}$ are the reference values of ideal-gas

enthalpy and ideal-gas entropy, respectively, for the ith component at the reference conditions (T_o, ρ_o).

Since the ideal part is easily obtained from the knowledge of the ideal-gas isobaric heat capacity functions of the components, the modeling effort is associated in particular with the residual part a_m^R. For the development of an EoS dedicated to a mixture, two methods are mainly available for this part:

- the *multi-fluid* approach, independently proposed by Tillner-Roth [1, 2] and Lemmon [3] and developed with further studies [4–7], that works with a linear combination of the reduced residual Helmholtz energy of the pure components and adds a departure function. Such a procedure requires the EoSs for all the pure fluids composing the mixture, and this restricts the applicability of the method. Moreover, experimental data are required for the regression of the departure function;
- the *one-fluid* approach, usually based on extended corresponding states (ECS) in various versions and applications [8–15], in which the mixture behavior at fixed composition is considered equivalent to that of a pseudo-pure fluid whose parameters are obtained from a combination of the pure-component parameters through empirical mixing rules. Such mixing rules also have binary interaction parameters that are regressed on mixture experimental data.

An improved version of the ECS technique was presented in Refs. 16 and 17. Even if in those studies the basic framework of the model was retained, the scale factors, i.e., the functions distorting the independent variables of the EoS of the reference fluid to meet the surface of the target system, were directly obtained as continuous functions in neural network form through regression on experimental data. The ECS requirement to choose a reference fluid conformal with the system of interest and having a high-accuracy dedicated equation of state (DEoS) is anyway present, and it can constitute a limiting condition for the model application.

Moving from such studies, a new modeling technique was presented for pure fluids in Ref. 18, in which a preliminary EoS for the target fluid itself is assumed as a reference instead of the equation for the reference fluid; in this way, the reference fluid becomes obsolete. The starting EoS, that can be, for instance, a simple cubic equation, is then improved and extended through the application of scale factors that correct the discrepancies between the initial model and experimental data by distorting the independent variables of the equation. For this reason, the method was labeled as "extended equation of state" (EEoS).

Again, the scale factors are expressed as continuous functions by a neural network trained on experimental data. Since this technique is a combination of the EEoS method with neural networks (NN), it was concisely indicated as "EEoS-NN model".

The present work deals with the extension of the method proposed for pure fluids in Ref. 18 to mixtures.

2. SUMMARY OF THE EEoS-NN MODEL FOR PURE FLUIDS

In this section, the basic elements of the EEoS-NN modeling technique for pure fluids are summarized to give the basis for the extension of the method to mixtures. In a former paper [18], the EEoS-NN framework for pure fluids was fully discussed and reference is made to that work for further modeling details, while the ECS method and its enhancements were dealt with in Refs. 16 and 17.

The background of the proposed technique is constituted by the ECS method, which states that for two conformal fluids, denoted with the subscripts 0 and j, the fundamental equation holds:

$$a_j^{\mathrm{R}}\left(T_j, \rho_j\right) = a_0^{\mathrm{R}}\left(T_0, \rho_0\right) = a_0^{\mathrm{R}}\left(T_j / f_j, \rho_j h_j\right) \tag{4}$$

where the scale factors f_j and h_j can be expressed as

$$f_j = \frac{T_{\mathrm{c},j}}{T_{\mathrm{c},0}}\,\theta_j\left(T_j, \rho_j\right) \tag{5}$$

$$h_j = \frac{\rho_{\mathrm{c},0}}{\rho_{\mathrm{c},j}}\,\phi_j\left(T_j, \rho_j\right) \tag{6}$$

The shape functions θ_j and ϕ_j are fluid-specific functions in the independent variables temperature and density of the fluid of interest. In case that the conformality condition is exactly fulfilled for the fluids, the shape functions are identically equal to 1 and the scale factors coincide with the critical constant ratios; otherwise, the shape functions account for the departure from perfect similarity in terms of the corresponding-states principle.

The goal of the ECS method is to represent the thermodynamic behavior of the target fluid j with respect to the reference fluid 0, for which a DEoS must be available. Once the shape functions of the target fluid are determined, all of its thermodynamic properties can be obtained through differentiation of the fundamental equation, Eq. (4), with respect to temperature and/or density.

In order to overcome the basic requirements of the ECS method, which are the conformality between target and reference fluids and the availability of a fundamental DEoS for the reference fluid, an EEoS model has been proposed [18] avoiding these constraints. Instead of a "reference fluid," only a "reference equation" for the target fluid itself is needed for the application of the technique. Any EoS in a fundamental form can be assumed, but considering the general requirement that the model represents the mixture behavior in any thermodynamic region, including the coexistence surfaces, only the fundamental form $a(T, \rho)$ can be considered. A Soave–Redlich–Kwong (SRK) cubic EoS [19, 20] can for instance be assumed, since it is possible to set it up for any fluid in an almost predictive mode. The precision of the reference EoS is then enhanced, or "extended," through the application of the shape functions to its independent variables maintaining the formalism of Eq. (4), see Appendix. For sake of clarity, in the following the term "reference equation" is replaced with the term "basic equation."

In the proposed method [18], the analytical form of the shape functions $\theta_j(T_j, \rho_j)$ and $\phi_j(T_j, \rho_j)$ is expressed through a multi-layer feed-forward neural network (MLFN), that is, a universal function approximator [21]. The values of the coefficients of the neural network are obtained through a regression procedure, indicated as "training," which forces the model to represent known values of experimentally accessible thermodynamic quantities for the target fluid, aimed at obtaining a precise multiproperty representation of the fluid itself.

3. MATHEMATICAL FORMULATION OF THE EEoS-NN MODEL FOR MIXTURES

3.1. EEoS Framework

For the case of a mixture m with C components, the EEoS fundamental equation for a pure fluid, Eq. (4), is rewritten in the independent variables T_m, ρ_m, and $\bar{z}$ $(=z_1, \ldots, z_{C-1})$:

$$a_m^R(T_m, \rho_m, \bar{z}) = a_0^R(T_0, \rho_0, \bar{z}) \tag{7}$$

where $\bar{z}$ is the array of mole fractions and the subscript 0 indicates the basic EoS assumed for the target mixture. It should be noted that in this case, in contrast with the customary formalism of the ECS format for mixtures [11–13, 17], the equation assumed as a reference also depends on the mixture composition.

In order to fulfill Eq. (7), the independent variables T_0 and ρ_0 of the mixture basic EoS have to be "distorted" through the scale factor func-

tions f_m and h_m, which are individually determined for the mixture of interest:

$$T_0 = \frac{T_m}{f_m(T_m, \rho_m, \bar{z})} \tag{8}$$

$$\rho_0 = \rho_m h_m(T_m, \rho_m, \bar{z}) \tag{9}$$

The mixture shape functions θ_m and ϕ_m can be introduced to describe f_m and h_m:

$$f_m = \frac{T_{c,m}}{T_{c,0}} \theta_m(T_m, \rho_m, \bar{z}) \tag{10}$$

$$h_m = \frac{\rho_{c,0}}{\rho_{c,m}} \phi_m(T_m, \rho_m, \bar{z}) \tag{11}$$

but, since the target and reference systems are the same, the ratios of their pseudo-critical temperatures and densities are equal to 1 and consequently the scale factors and the shape functions coincide:

$$f_m = f_m(T_m, \rho_m, \bar{z}) = \theta_m(T_m, \rho_m, \bar{z}) \tag{12}$$

$$h_m = h_m(T_m, \rho_m, \bar{z}) = \phi_m(T_m, \rho_m, \bar{z}) \tag{13}$$

Therefore, in this case the mixing rules for the critical parameters, that would be unavoidable for a multi-fluid approach, are not required. The fundamental equation of the mixture EEoS model is finally expressed as

$$a_m^R(T_m, \rho_m, \bar{z}) = a_0^R\left(T_m / f_m, \rho_m h_m, \bar{z}\right) \tag{14}$$

Once the scale factor functions f_m and h_m for the target mixture are known, any other thermodynamic function can be obtained from this equation just through derivatives with respect to temperature, density, and mole fraction; in fact, Eq. (14) represents a fundamental equation of state for the target mixture. The mathematical relations for the calculation of thermodynamic properties, given in the Appendix, are the same as those for the ECS model [11, 16, 17], but in the present case the equation for the reference fluid is substituted by the basic equation for the mixture itself.

A significant formal difference with the ECS framework is given by the partial molar fugacity coefficient $\hat{\varphi}_i$ for the ith mixture component, that in EEoS format reads

$$\ln\hat{\varphi}_i = \left[\frac{\partial\,(n\ln\varphi_{\mathrm{m}})}{\partial n_i}\right]_{P_{\mathrm{m}},T_{\mathrm{m}},n_{j\neq i}} = \ln\hat{\varphi}_{0,i} - \ln\left[1+u_0^{\mathrm{R}}F_\rho + Z_0^{\mathrm{R}}\left(1+H_\rho\right)\right] + \ln\left(1+Z_0^{\mathrm{R}}\right) + u_0^{\mathrm{R}}\left(F_{n_i}+F_\rho\right) + Z_0^{\mathrm{R}}\left(H_{n_i}+H_\rho\right) \tag{15}$$

where $\hat{\varphi}_{0,i}$ is the partial molar fugacity coefficient calculated by the basic EoS, n_i is the number of moles of component i in the system, n is the total number of moles, $Z_0^{\mathrm{R}} = Z_0 - 1$ and $u_0^{\mathrm{R}} = U_0^{\mathrm{R}}/RT_0$ are, respectively, the residual compressibility factor and the reduced residual internal energy both obtained from the basic equation, and F_ρ and H_ρ are the logarithmic derivatives of the scale factors with respect to density. The terms F_{n_i} and H_{n_i} are the logarithmic derivatives of the scale factors with respect to the number of moles n_i and they can be expressed as

$$F_{n_i} = \left(\frac{\partial f_{\mathrm{m}}}{\partial n_i}\right)_{T_{\mathrm{m}},\rho_{\mathrm{m}},n_{j\neq i}}\left(\frac{n_i}{f_{\mathrm{m}}}\right) = \frac{1}{f_{\mathrm{m}}}\left\{\left(\frac{\partial f_{\mathrm{m}}}{\partial z_i}\right)_{T_{\mathrm{m}},\rho_{\mathrm{m}},z_{j\neq i}} - \sum_{k=1}^{C-1}\left[z_k\left(\frac{\partial f_{\mathrm{m}}}{\partial z_k}\right)_{T_{\mathrm{m}},\rho_{\mathrm{m}},z_{j\neq k}}\right]\right\} \tag{16}$$

$$H_{n_i} = \left(\frac{\partial h_{\mathrm{m}}}{\partial n_i}\right)_{T_{\mathrm{m}},\rho_{\mathrm{m}},n_{j\neq i}}\left(\frac{n_i}{h_{\mathrm{m}}}\right) = \frac{1}{h_{\mathrm{m}}}\left\{\left(\frac{\partial h_{\mathrm{m}}}{\partial z_i}\right)_{T_{\mathrm{m}},\rho_{\mathrm{m}},z_{j\neq i}} - \sum_{k=1}^{C-1}\left[z_k\left(\frac{\partial h_{\mathrm{m}}}{\partial z_k}\right)_{T_{\mathrm{m}},\rho_{\mathrm{m}},z_{j\neq k}}\right]\right\} \tag{17}$$

The equations representing the various thermodynamic functions resulting from the mixture model are always a combination of residual functions calculated from the mixture basic EoS and of derivatives of the scale functions f_{m} and h_{m}. The calculation of such properties from the EEoS model requires the availability of a basic EoS for the mixture itself and of the individual scale functions for the target mixture:

$$f_{\mathrm{m}} = f_{\mathrm{m}}\left(T_{\mathrm{m}}, \rho_{\mathrm{m}}, \bar{z}\right) \tag{18}$$

$$h_{\mathrm{m}} = h_{\mathrm{m}}\left(T_{\mathrm{m}}, \rho_{\mathrm{m}}, \bar{z}\right) \tag{19}$$

which, unlike the pure fluid case [18], depend also on the mixture molar composition.

In the following it will be discussed how to supply the basic EoS for the target mixture and then how to obtain the functional forms of the mixture scale factor functions.

3.2. Basic EoS for the Target Mixture

The application of the EEoS model is not restricted to a particular choice of the functional form for the mixture basic EoS, but only at the condition that it is expressed as a fundamental equation in terms of Helmholtz energy as a function of temperature, density, and mole fraction. A different selection of the EoS modifies only the analytical developments concerning the EoS itself, while the rest of the EEoS model is left unmodified. For instance, it could be possible to proceed to an enhancement of an existing DEoS for the target mixture after new data sets are made available in the literature: in this case such a DEoS could be assumed as the basic EoS for the EEoS model and an improved representation of the thermodynamic surface for the mixture would be developed from it.

An opposite situation is found when no DEoS has been previously developed for the studied mixture or even its components have not yet been thermodynamically represented. In this case it is convenient to choose a very simple and general form for the basic EoS in order to allow the representation of practically any mixture in a predictive mode, even if the mixture is represented with low accuracy. A cubic EoS is a convenient choice for these conditions.

In the first part of this work [18], the SRK cubic EoS [19, 20] with the Peneloux volume translation [22] was assumed as the basic EoS and the same choice is maintained here for the description of mixtures. As shown in Ref. 18, the SRK equation can be easily converted into a fundamental form giving

$$a_0^{\mathrm{R}} = -\ln\left[1 + (c-b)\,\rho_0\right] - \frac{a_{\mathrm{SRK}}}{RT_0 b}\ln\left[\frac{1+(c+b)\,\rho_0}{1+c\rho_0}\right] \tag{20}$$

For a mixture, the coefficients a_{SRK}, b, and the volume translation parameter c in Eq. (20) depend also on molar composition and are obtained from the corresponding parameters for the pure components by suitable mixing rules. The conventional van der Waals mixing rules are assumed here because of their wide applicability together with a very simple formulation:

$$a_{\mathrm{SRK}} = \sum_{i=1}^{C}\sum_{j=1}^{C} z_i z_j \left(a_i a_j\right)^{1/2}\left(1-k_{ij}\right) \tag{21}$$

$$b = \sum_{j=1}^{C} z_j b_j \tag{22}$$

$$c = \sum_{j=1}^{C} z_j c_j \tag{23}$$

where a_j, b_j, and c_j are the SRK parameters of the jth pure component of the mixture and z_j is its mole fraction. Details on the substance-specific parameters are reported in Ref. 18; here it is recalled that only the parameters b_j and c_j are constant, whereas a_j is a function of temperature and acentric factor ω_j.

The binary interaction coefficients k_{ij} in Eq. (21) are usually regressed from mixture experimental data; in the EEoS model they may be set equal to zero, since the resulting deviations of a totally predictive cubic EoS can be recovered by the action of the mixture scale factors, particularly in the case of moderately deviating mixtures.

All the thermodynamic properties of the basic equation are obtained from differentiation of Eq. (20) with respect to temperature and density, following the classical relations for fundamental EoS [1, 2, 23]. These quantities, denoted by the subscript 0, represent the contributions of the basic equation which enter into the expressions for the property calculation borrowed from the ECS framework [16, 17].

In particular, for the representation of the partial molar fugacity coefficient $\hat{\varphi}_i$, Eq. (15), the partial molar fugacity coefficient $\hat{\varphi}_{0,i}$ expressed from the basic EoS is calculated as

$$\begin{aligned}\ln\hat{\varphi}_{0,i} = &-\ln\{Z_0[1+(c-b)\rho_0]\} - \frac{a_{\mathrm{SRK}}}{RT_0 b}\left(1+\frac{\bar{a}_{\mathrm{SRK},i}}{a_{\mathrm{SRK}}}-\frac{\bar{b}_i}{b}\right)\\ &\times\ln\left[\frac{1+(c+b)\rho_0}{1+c\rho_0}\right] - \frac{(\bar{c}_i-\bar{b}_i)\rho_0}{1+(c-b)\rho_0} - \frac{a_{\mathrm{SRK}}\rho_0}{RT_0 b}\\ &\times\left[\frac{\bar{c}_i+\bar{b}_i}{1+(c+b)\rho_0}-\frac{\bar{c}_i}{1+c\rho_0}\right]\end{aligned} \tag{24}$$

with

$$\begin{aligned}\bar{a}_{\mathrm{SRK},i} &= \left[\frac{\partial(n a_{\mathrm{SRK}})}{\partial n_i}\right]_{T_0,\rho_0,n_{j\neq i}}\\ &= \begin{cases}\bar{a}_{\mathrm{SRK},1} = 2z_1a_1 + 2z_2(1-k_{12})(a_1a_2)^{1/2} - a_{\mathrm{SRK}}\\ \bar{a}_{\mathrm{SRK},2} = 2z_2a_2 + 2z_1(1-k_{12})(a_1a_2)^{1/2} - a_{\mathrm{SRK}}\end{cases}\end{aligned} \tag{25}$$

$$\bar{b}_i = \left[\frac{\partial(nb)}{\partial n_i}\right]_{T_0,\rho_0,n_{j\neq i}} = b_i \tag{26}$$

$$\bar{c}_i = \left[\frac{\partial(nc)}{\partial n_j}\right]_{T_0,\rho_0,n_{j\neq i}} = c_i \tag{27}$$

where the expressions for $\bar{a}_{\mathrm{SRK},1}$ and $\bar{a}_{\mathrm{SRK},2}$ in Eq. (25) are examples for a binary mixture.

3.3. Representation of the Scale Factors

For the analytical representation of the scale factor functions f_m and h_m of the target mixture, a general function approximator is integrated into the EEoS model with a procedure similar to that used in the first part of this work for pure fluids [18]. As in that case, the problem is to "spread" the functional form of the thermodynamic surface over known values of thermodynamic properties distributed on the surface itself. In fact, the new EEoS model includes a multiparameter function whose coefficients are obtained through an optimization procedure for which an objective function, defined as a sum of squares considering a number of thermodynamic quantities, has to be minimized.

The chosen neural network in the MLFN format is an effective and powerful function approximator [21] with an *a priori* known functional form, and it was formerly applied in a similar framework for modeling the thermodynamic properties [16–18, 24, 25] and the transport properties [26–29] of pure fluids and mixtures. The use of neural networks for the representation of the scale factor functions of the model is indicated by the name "EEoS-NN" given to the proposed technique. For the sake of brevity, the mathematical formulation of MLFN is only summarized here, but reference is made to the paper for pure fluids [18] where it is presented in detail.

The MLFN is applied to simultaneously represent the scale factor functions $f_m = f_m(T_m, \rho_m, \bar{z})$ and $h_m = h_m(T_m, \rho_m, \bar{z})$ as functions of the independent variables T_m, ρ_m, and $\bar{z}\ (=z_1, \ldots, z_{C-1})$, i.e., temperature, density, and $C-1$ mole fractions of the mixture of interest. In this architecture, schematically shown in Fig. 1, there are several neuron layers (*multilayer*) and the information goes in only one direction, from input to output (*feedforward*). The $I-1$ inputs U_i enter the $I-1$ neurons of the input layer, while the Ith neuron has a constant value equal to Bias1. The inputs U_i represent the independent variables of the problem: I is equal to 4 for a binary mixture, equal to 5 for a ternary mixture, and so on. The outputs S_1 and S_2 of the output layer are the dependent variables of the problem, i.e., the scale factors f_m and h_m; in the present case the number of neurons K in the output layer is equal to 2. The neural network application is easier if the inputs and outputs have the same range of values; therefore, the variables are scaled and compressed in an arbitrarily chosen range [0.05, 0.95] as explained in detail in Ref. 18.

The number of neurons J in the hidden layer can be varied by trial and error searching for the lowest value of the objective function to minimize, but it must be limited to avoid overfitting problems. In the present work, J was chosen equal to 11 for binary mixtures and equal to 7

for ternary mixtures. These values are a compromise between the accuracy of the equations and the computational speed. Considering the number of data used for the regression, such values are sufficiently low to avoid over-fitting. The last neuron of the hidden layer has a constant value indicated as Bias2.

The transfer function $g(x)$ converts the input signals to output for each neuron; in the present work an arctangent function normalized in the range [0, 1] was chosen;

$$g(x) = \frac{1}{\pi}\arctan(\gamma x) + \frac{1}{2} \tag{28}$$

with $\gamma = 0.5$. The analytical form of the present MLFN is essentially represented by

$$U_I = \text{Bias1} \tag{29}$$

$$H_j = g\left(\sum_{i=1}^{I} w_{ij} U_i\right) \quad \text{with } 1 \leqslant j \leqslant J \tag{30}$$

$$H_{J+1} = \text{Bias2} \tag{31}$$

$$S_k = g\left(\sum_{j=1}^{J+1} w_{jk} H_j\right) \quad \text{with } 1 \leqslant k \leqslant K \tag{32}$$

where the g function in Eqs. (30) and (32) is given by Eq. (28).

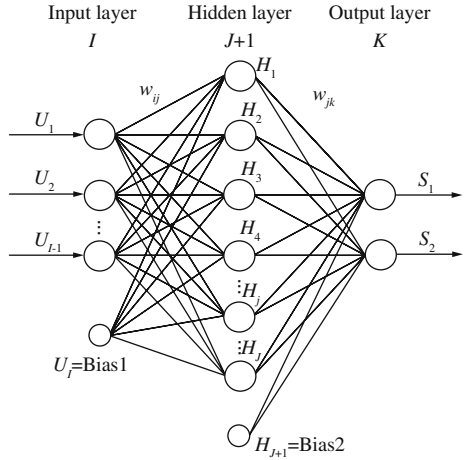

Fig. 1. General topology of a three-layer feedforward neural network.

The parameter arrays $\bar{w}_{ij}$ and $\bar{w}_{jk}$ in the function approximator have to be regressed by minimization of an objective function calculated from experimental data for the target mixture, as will be explained in the following section. Since the method is totally heuristic, it is essential that the experimental data are as evenly distributed as possible.

Once the training procedure has been completed and the values of the parameters are known, all the elements of the EEoS-NN are available and the thermodynamic properties of the mixture of interest are easily calculated through simple mathematical operations.

For an example of the procedure for the calculation of a thermodynamic property function according to the present model, reference can be made to the analogous case for pure fluids described in Section 4.3 of the first part of this work [18]. Only the mole fraction variables are to be added in that explanation. The corresponding formalism is reported in the Appendix. The calculation of the vapor–liquid equilibrium (VLE) requires the solution of the equation system,

$$\begin{cases} x_1^{\text{sat}}\hat{\varphi}_1^{\text{sl}} = y_1^{\text{sat}}\hat{\varphi}_1^{\text{sv}} \\ \quad\vdots \\ x_i^{\text{sat}}\hat{\varphi}_i^{\text{sl}} = y_i^{\text{sat}}\hat{\varphi}_i^{\text{sv}} \\ \quad\vdots \\ x_C^{\text{sat}}\hat{\varphi}_C^{\text{sl}} = y_C^{\text{sat}}\hat{\varphi}_C^{\text{sv}} \end{cases} \tag{33}$$

where the superscript sat denotes a value at saturation, the superscripts sl and sv stand for saturated liquid and saturated vapor conditions, while the arrays $\bar{x}^{\text{sat}}$ and $\bar{y}^{\text{sat}}$ are the mole fractions of the liquid and of the vapor phase in equilibrium, respectively. For each component i the partial molar fugacity coefficient $\hat{\varphi}_i$ is calculated from Eq. (15) for the saturated liquid at $\left(T, \rho^{\text{sl}}, \bar{x}^{\text{sat}}\right)$ conditions and for the saturated vapor at $\left(T, \rho^{\text{sv}}, \bar{y}^{\text{sat}}\right)$ conditions. The densities of the two phases are obtained at given temperature, pressure, and composition conditions as density values for which the calculated pressure equals the assigned value. Depending on the type of VLE calculation considered, the unknowns of the equation system, Eq. (33), can be chosen among temperature, pressure, liquid phase composition, and vapor phase composition.

4. TRAINING OF THE EEoS-NN MODEL

The training of an EEoS-NN model aims at the determination of the mixture scale factor functions f_{m} and h_{m} over the whole $(T, \rho, \bar{z})$ range

of interest through an optimization procedure that uses the available data of the experimentally accessible thermodynamic quantity as input.

The main goal of the present work is to verify the effectiveness of the proposed modeling technique and its capability in representing the thermodynamic surfaces of mixtures. Therefore, similarly to what was done in the first part for pure fluids [18], generated values of thermodynamic properties were chosen instead of experimental data, because the first ones can be regularly distributed over the whole range of interest and they are affected neither by experimental uncertainty nor by error noise. In this way, the heuristic method can work under the most favorable conditions, since the drawbacks of experimental data are avoided. The evaluation of the results is not affected by the accuracy level of the data in this preliminary test.

Five binary and two ternary mixtures of haloalkanes were considered, and for all of them, the DEoSs used for data generation were taken from Ref. 5. The critical constants and the SRK parameters for the pure fluids relevant as components of the selected mixtures are reported in Table I together with their literature references.

In a first step, only density data in the form $(T, P, \rho, \bar{z})$ and covering the vapor, liquid, and supercritical regions, together with VLE data in the form $(T, P^{\text{sat}}, \bar{x}^{\text{sat}}, \rho^{\text{sl}}, \bar{y}^{\text{sat}}, \rho^{\text{sv}})$, were used as inputs for the regression. The VLE data are necessary to locate the bubble and dew surfaces of the mixture.

A grid of calculated densities was generated in the independent variables $T, P, \bar{z}$ with a constant step for each variable inside the respective range. This pseudo-experimental data set was subdivided into a training set and a validation set. The first one was obtained extracting a subset of values from the original set, and the second one was composed of the remaining values. The data of the training set were assumed for the regression of the mixture-specific equations, while the validation data were used to check the performances of the obtained models. Following similar criteria, sets of training and validation VLE data were produced for the

Table I. Critical Constants and Parameters for the Pure Fluids Involved in the Considered Binary and Ternary Mixtures

Fluid	T_c (K)	P_c (MPa)	ω	c (L·mol^{-1})	Ref.
R32	351.255	5.782	0.2768	1.29133×10^{-2}	30
R125	339.33	3.629	0.30349	7.79698×10^{-3}	31
R134a	374.18	4.05629	0.32689	1.13412×10^{-2}	32
R143a	346.04	3.7756	0.26113	1.34996×10^{-2}	33

whole coexistence locus in the considered temperature range. Moreover, values of several thermodynamic properties were generated for each point of the validation set, in order to verify the behavior of the equations also with respect to such quantities.

The number of data and their range for each considered mixture are reported in Table II. The data are distributed in three main thermodynamic regions, which are the liquid phase (denoted by l), the vapor phase (denoted by v), and the supercritical region (denoted by sc). In this work the supercritical region is conventionally identified as the thermodynamic region at temperatures higher than the pseudocritical temperature and pressures higher than the pseudocritical pressure, calculated by the mixing rules of Tillner-Roth et al. [5].

For the training step an objective function f_{ob}, accounting for the deviations between the model and the data, has to be defined for each of the thermodynamic quantities on which the equation is regressed. The variables of the f_{ob} function are the parameters $\bar{w}_{ij}$ and $\bar{w}_{jk}$, whose values are to be found through a minimization procedure of the f_{ob} function.

Table II. Characteristics of the Generated Data for the Considered Mixtures

Mixture	T Range (K)	P Range (MPa)	z_1 Range	z_2 Range
R32/R125	250–400	0.3–8.0	0.01–0.98	–
R32/R134a	250–400	0.3–8.0	0.01–0.98	–
R125/R134a	250–400	0.3–8.0	0.01–0.98	–
R125/R143a	250–400	0.3–8.0	0.01–0.98	–
R143a/R134a	250–400	0.3–8.0	0.01–0.98	–
R32/R125/R134a	250–400	0.3–8.0	0.01–0.98	0.01–0.98
R125/R143a/R134a	250–400	0.3–8.0	0.01–0.98	0.01–0.98

	Training NPT					Validation NPT				
	$P, \rho, T, \bar{z}$				VLE	Each of nine properties [a]				VLE
	sc	l	v	Overall		sc	l	v	Overall	
R32/R125	137	388	253	778	44	834	2305	1448	4587	115
R32/R134a	80	473	218	771	53	456	2822	1239	4517	140
R125/R134a	126	471	185	782	51	677	2815	1030	4522	133
R125/R143a	168	394	203	765	42	927	2391	1107	4425	113
R143a/R134a	114	489	183	786	53	612	2893	1020	4525	136
R32/R125/R134a	101	311	187	599	64	902	3382	1834	6118	354
R125/R143a/R134a	111	321	170	602	64	1101	3491	1479	6071	344

[a] Properties: Z^R, a^R, u^R, h^R, g^R, s^R, c_v^R, c_p^R, w.

In the present case, it was chosen to train the MLFN only on density values in the vapor, liquid, and supercritical regions, and on the liquid-vapor coexistence surface.

Considering a mixture of C components for which a set of NPT_Z density data and a set of NPT_φ VLE data are available, two objective functions can be defined:

$$f_{\mathrm{ob},Z^{\mathrm{R}}} = \frac{1}{\mathrm{NPT}_Z} \sum_{i=1}^{\mathrm{NPT}_Z} \left[\frac{\left(Z_{\mathrm{m}}^{\mathrm{R}}\right)_i^{\mathrm{exp}} - \left(Z_{\mathrm{m}}^{\mathrm{R}}\right)_i^{\mathrm{calc}}}{\left(Z_{\mathrm{m}}^{\mathrm{R}}\right)_i^{\mathrm{exp}}} \right]^2 \tag{34}$$

$$f_{\mathrm{ob},\varphi-\varphi} = \frac{1}{\mathrm{NPT}_\varphi} \sum_{j=1}^{\mathrm{NPT}_\varphi} \sum_{k=1}^{C} \left[\left(\ln x_k^{\mathrm{sat}} + \ln \hat{\varphi}_k^{\mathrm{sl}} \right)_j - \left(\ln y_k^{\mathrm{sat}} + \ln \hat{\varphi}_k^{\mathrm{sv}} \right)_j \right]^2 \tag{35}$$

for the residual compressibility factor and coexistence, respectively. The superscripts exp and calc stand for experimental and calculated values. In Eq. (35) x_k^{sat} and y_k^{sat} are experimental values, while $\hat{\varphi}_k^{\mathrm{sl}}$ and $\hat{\varphi}_k^{\mathrm{sv}}$ are calculated through the EEoS-NN model at the experimental conditions $\left(T, \rho^{\mathrm{sl}}, \bar{x}^{\mathrm{sat}}\right)$ and $\left(T, \rho^{\mathrm{sv}}, \bar{y}^{\mathrm{sat}}\right)$. Since in the present study only generated values were considered instead of real experimental data, the term "experimental value" refers to values generated from the corresponding DEoS in Ref. 5.

The training step aims at the minimization of an overall objective function $f_{\mathrm{ob},ov}$ obtained as a combination of the ones for density and coexistence. The two contributions are differently weighted in the overall function by means of the coefficient ξ_1:

$$f_{\mathrm{ob},ov} = \xi_1 \; f_{\mathrm{ob},Z^{\mathrm{R}}} + (1 - \xi_1) \; f_{\mathrm{ob},\varphi-\varphi} \tag{36}$$

In this case, the value of the coefficient ξ_1 satisfactorily balancing the two contributions was set to 0.8. The application of the training procedure to the generated data gave a mixture-specific equation in EEoS-NN format for each of the target mixtures reported in Table II.

In a second step of the study, the EEoS-NN model was regressed assuming an objective function which includes, besides the unavoidable density and VLE data, some caloric quantities such as the isochoric heat capacity C_v, the isobaric heat capacity C_p, and the speed of sound w. The overall objective function $f_{\mathrm{ob},ov}$ for this multiproperty fitting is again calculated as the sum of two contributions, but the first one now reads

$$f_{\mathrm{ob},1} = \frac{1}{P \cdot \mathrm{NPT}_1} \sum_{p=1}^{P} \xi_p \sum_{i=1}^{\mathrm{NPT}_1} \left[\frac{(m_{\mathrm{m}})_i^{\mathrm{exp}} - (m_{\mathrm{m}})_i^{\mathrm{calc}}}{(m_{\mathrm{m}})_i^{\mathrm{exp}}} \right]_p^2 \tag{37}$$

In Eq. (37), the pth property m alternatively represents the residual compressibility factor Z^{R}, the reduced residual isochoric heat capacity c_v^{R}, the reduced residual isobaric heat capacity c_p^{R}, and the speed of sound w; in this case P is equal to 4. Each of the four mentioned properties has a training set containing NPT_1 values and its contribution is weighted in the summation according to the individual factor ξ_p.

The second component $f_{\mathrm{ob},\varphi-\varphi}$ of the objective function is represented by Eq. (35) and the two contributions are combined together giving

$$f_{\mathrm{ob},ov} = \xi_2 \; f_{\mathrm{ob},1} + (1-\xi_2) \; f_{\mathrm{ob},\varphi-\varphi} \tag{38}$$

where the coefficient ξ_2 has to be properly chosen; in this study it was set equal to 0.8 again.

In both cases the training of the MLFN is obtained from the minimization of either Eq. (36) or Eq. (38) through a conventional gradient descent technique [34].

The main purposes of the present study are the test and analysis of capability and performances of the proposed modeling method. Therefore, the numerical details, i.e., the parameters $\bar{w}_{ij}$ and $\bar{w}_{jk}$, of the functional forms obtained for the studied systems are reported in Table III for only a couple of mixtures for the convenience of the reader. In fact, they have a limited interest for practical applications since DEoSs already exist for all the considered mixtures [5].

5. VALIDATIONS

The main requirement for an EoS is the capability to accurately represent any thermodynamic property. In fact, all thermodynamic surfaces can be obtained by differentiation of the residual part $a_{\mathrm{m}}^{\mathrm{R}}(T_{\mathrm{m}}, \rho_{\mathrm{m}}, \bar{z})$ of a fundamental Helmholtz energy model, as for instance the residual compressibility factor $Z_{\mathrm{m}}^{\mathrm{R}}(T_{\mathrm{m}}, \rho_{\mathrm{m}}, \bar{z})$, the reduced residual internal energy $u_{\mathrm{m}}^{\mathrm{R}}(T_{\mathrm{m}}, \rho_{\mathrm{m}}, \bar{z})$, the reduced residual entropy $s_{\mathrm{m}}^{\mathrm{R}}(T_{\mathrm{m}}, \rho_{\mathrm{m}}, \bar{z})$, the reduced residual enthalpy $h_{\mathrm{m}}^{\mathrm{R}}(T_{\mathrm{m}}, \rho_{\mathrm{m}}, \bar{z})$, the reduced residual Gibbs energy $g_{\mathrm{m}}^{\mathrm{R}}(T_{\mathrm{m}}, \rho_{\mathrm{m}}, \bar{z})$, etc.

The performance of the obtained EEoS-NN models in representing such surfaces was verified in a validation step. As explained in Section 4, data generated from literature DEoSs for the studied mixtures were used for this purpose, considering them as "true" experimental values. In this way the drawbacks coming from the experimental uncertainty and the uneven distribution of literature experimental data in the range of validity are avoided.

Table III. Parameters of the EEoS-NN Equations for Two Considered Mixtures

R32/R125						R125/R143a/R134a					
I	4		Bias1	1.00		I	5		Bias1	1.00	
J	11		Bias2	1.00		J	7		Bias2	1.00	
K	2		A_{min}	0.05		K	2		A_{min}	0.05	
γ	0.5		A_{max}	0.95		γ	0.5		A_{max}	0.95	
$V_{1,min} \equiv T_{min}$	250 K		$V_{1,max} \equiv T_{max}$	400 K		$V_{1,min} \equiv T_{min}$	250 K		$V_{1,max} \equiv T_{max}$	400 K	
$V_{2,min} \equiv \rho_{min}$	0.06 mol·L^{-1}		$V_{2,max} \equiv \rho_{max}$	21.70 mol·L^{-1}		$V_{2,min} \equiv \rho_{min}$	0.060 mol·L^{-1}		$V_{2,max} \equiv \rho_{max}$	21.804 mol·L^{-1}	
$V_{3,min} \equiv z_{1,min}$	0.00		$V_{3,max} \equiv z_{1,max}$	1.00		$V_{3,min} \equiv z_{1,min}$	0.00		$V_{3,max} \equiv z_{1,max}$	1.00	
$W_{1,min} \equiv \theta_{min}$	0.6		$W_{1,max} \equiv \theta_{max}$	1.4		$V_{4,min} \equiv z_{2,min}$	0.00		$V_{4,max} \equiv z_{2,max}$	1.00	
$W_{2,min} \equiv \phi_{min}$	0.6		$W_{2,max} \equiv \phi_{max}$	1.4		$W_{1,min} \equiv \theta_{min}$	0.6		$W_{1,max} \equiv \theta_{max}$	1.4	
						$W_{2,min} \equiv \phi_{min}$	0.6		$W_{2,max} \equiv \phi_{max}$	1.4	
i	j	w_{ij}	i	j	w_{ij}	i	j	w_{ij}	j	k	w_{jk}
1	1	6.58428	4	9	1.14992	1	1	6.35829	1	1	2.39430
2	1	10.3152	1	10	−0.436056	2	1	−2.52168	2	1	1.15201
3	1	0.814873	2	10	3.35685	3	1	−6.80357	3	1	−17.7230
4	1	2.28105	3	10	−1.49919	4	1	−2.05343	4	1	1.03240
1	2	2.44133	4	10	3.03133	5	1	−10.9248	5	1	14.5853
2	2	0.269414	1	11	2.50812	1	2	−1.82751	6	1	10.3455
3	2	2.61651	2	11	4.44018	2	2	−11.0058	7	1	−8.69174
4	2	1.99816	3	11	−1.01839	3	2	−0.395631	8	1	−1.23912
1	3	−2.70715	4	11	−4.34660	4	2	−0.106151	1	2	−6.38606
2	3	1.23786				5	2	6.16792	2	2	−6.65546
3	3	−4.78297	j	k	w_{jk}	1	3	−1.20288	3	2	10.7842
4	3	−5.66760	1	1	−33.4498	2	3	−5.76217	4	2	8.36261
1	4	−0.465592	2	1	14.3559	3	3	1.38934	5	2	24.2427
2	4	0.125346	3	1	26.5665	4	3	−0.999631	6	2	1.12449

Table III. *Continued*

R32/R125						R125/R143a/R134a					
3	4	1.71910	4	1	−8.09493	5	3	−5.47576	7	2	−4.48644
4	4	−0.404574	5	1	8.61892	1	4	3.25677	8	2	−7.80621
1	5	−0.135371	6	1	13.9744	2	4	22.5494			
2	5	1.41579	7	1	−2.26905	3	4	−0.296072			
3	5	1.44208	8	1	5.46675	4	4	0.267324			
4	5	−0.984205	9	1	−2.50925	5	4	−1.74245			
1	6	4.48318	10	1	−2.89316	1	5	−3.80325			
2	6	14.1739	11	1	1.05538	2	5	−13.1640			
3	6	1.43756	12	1	5.20694	3	5	−0.586427			
4	6	0.454792	1	2	−0.338255	4	5	−0.163099			
1	7	−0.0400275	2	2	5.65861	5	5	−0.069184			
2	7	−4.47537	3	2	2.15018	1	6	1.25384			
3	7	−0.579075	4	2	−4.93073	2	6	−6.70487			
4	7	3.02816	5	2	0.717927	3	6	4.09364			
1	8	−0.0459610	6	2	−20.7335	4	6	1.41696			
2	8	−4.55918	7	2	11.4056	5	6	−11.9152			
3	8	0.340360	8	2	−36.2618	1	7	−3.95723			
4	8	2.22624	9	2	25.2766	2	7	−7.11796			
1	9	0.215355	10	2	1.59063	3	7	−2.40258			
2	9	−4.68901	11	2	1.43788	4	7	1.69038			
3	9	1.14628	12	2	17.4495	5	7	−5.75557			

In this work, the percentage deviation Δ (%) and the percentage average absolute deviation AAD (%) with respect to a data base of NPT values are evaluated as

$$\Delta\ (\%) = 100\,\frac{m^{\exp} - m^{\mathrm{calc}}}{m^{\exp}} \tag{39}$$

$$\mathrm{AAD}\ (\%) = \frac{1}{\mathrm{NPT}} \sum_{i=1}^{\mathrm{NPT}} |\Delta\ (\%)|_i \tag{40}$$

where m indicates a thermodynamic function, as for instance Z^{R}, a^{R}, u^{R}, h^{R}, etc. When dealing with VLE data, the deviation in the composition of the coexisting phases is calculated as

$$\Delta_j = z_j^{\exp} - z_j^{\mathrm{calc}} \tag{41}$$

where z_j represents the mole fraction of the jth component in the liquid or vapor phase; in these cases the AAD for each phase is reported in the tables as a mean value of the AADs of the components:

$$\mathrm{AAD} = \frac{1}{C} \sum_{j=1}^{C} \frac{1}{\mathrm{NPT}} \sum_{i=1}^{\mathrm{NPT}} \left|\Delta_j\right|_i \tag{42}$$

For the present validation step, the assumed independent variables are the temperature T_{m}, the pressure P_{m}, and the mole fraction array $\bar{z}$; therefore, a procedure of inversion is required for the calculation of the density ρ_{m}, which is an independent variable of the fundamental equations in terms of Helmholtz energy.

Two VLE cases are considered for the validation at saturation conditions:

- the "Bubble P" case, for which the inputs are the temperature and the liquid phase compositions, while the variables to be calculated are the pressure and the vapor phase compositions;
- the "Dew P" case, for which the inputs are the temperature and the vapor phase compositions, while the variables to be calculated are the pressure and the liquid phase compositions.

5.1. Basic Accuracy of a Cubic One-Fluid-Model EoS: Case of SRK with Volume Translation

First of all, the SRK cubic EoS [19, 20] with the Peneloux volume translation [22], applied to mixtures as a one-fluid model, was validated with respect to the generated data in the validation sets for properties involving only first-order derivatives of a_m^R with respect to temperature or density. The physical constants and the coefficients reported in Table I were used for the components, whereas the binary interaction parameters k_{ij} were set to zero. The SRK performances represent the "starting point" of the proposed modeling technique; in fact, the discrepancies between the data and the predictions of this equation are corrected through the application of the scale factors.

Results for the SRK equation with $k_{ij}=0$ are reported in Table IV for the considered binary and ternary mixtures. The performances are rather homogeneous for all the systems, but the prediction errors for the properties depending on first derivatives of the residual Helmholtz energy range to several parts per cent. The worse performances are found for properties involving only temperature derivatives like u_m^R and s_m^R, particularly, in the vapor region where the AADs can generally exceed 10%.

Table V shows the accuracy of the SRK model for the thermodynamic properties depending on second and cross derivatives of a_m^R. The results for isochoric and isobaric heat capacities, and for the speed of sound are similar for binary and ternary mixtures, but are worse than those obtained for first-order properties, see Table IV. In particular, the residual heat capacities show very high deviations, which are considerably reduced when also the ideal part of the properties is considered. The errors are rather homogeneous in all the regions for the heat capacities, but for the speed of sound the good results in the vapor phase are in contrast with the poor performance in the liquid phase, where a mean deviation of about 25% is obtained. This is due to the ideal-gas contribution for speed of sound that prevails in the vapor phase.

Table VI shows the SRK model performance for the prediction of the properties at equilibrium conditions for binary and ternary mixtures. The bubble- and dew-point pressures and the phase compositions are predicted with acceptable accuracies, whereas the deviations for the densities at saturation are higher, with worse values for the saturated liquid density.

Considering the reported results, it can be concluded that from an overall point of view the accuracy of the SRK cubic EoS, using mixing rules set with $k_{ij}=0$, cannot be regarded as satisfactory.

Table IV. Accuracy of the SRK Equation for Thermodynamic Quantities Depending on First Derivatives of Residual Helmholtz Energy in the Three Main Thermodynamic Regions

	AAD (%)							
	sc	l	v	Overall	sc	l	v	Overall
Mixture	Z_m^R				s_m^R			
R32 + R125	3.64	0.86	3.28	2.13	3.89	2.11	17.65	7.34
R32 + R134a	4.81	0.82	4.43	2.21	5.00	3.34	22.35	8.72
R125 + R134a	5.11	0.78	2.08	1.72	2.66	2.09	13.74	4.83
R125+R143a	6.35	0.90	3.09	2.59	2.99	2.07	12.96	4.99
R143a + R134a	6.29	0.82	4.08	2.29	3.25	3.08	18.07	6.48
Mean	**5.26**	**0.83**	**3.42**	**2.19**	**3.45**	**2.57**	**17.14**	**6.48**
R32 + R125 + R134a	4.12	0.80	3.56	2.12	3.57	2.55	19.24	7.70
R125 + R143a + R134a	5.93	0.80	2.83	2.22	2.88	2.12	14.25	5.21
Mean	**5.11**	**0.80**	**3.23**	**2.17**	**3.19**	**2.33**	**17.01**	**6.46**
	u_m^R				a_m^R			
R32 + R125	3.51	1.43	11.93	5.12	4.00	2.98	3.53	3.34
R32 + R134a	5.64	1.82	15.58	5.98	6.66	2.98	4.55	3.78
R125 + R134a	3.24	1.19	8.99	3.27	5.67	2.24	2.07	2.71
R125 + R143a	3.82	1.28	8.91	3.72	7.15	3.38	3.01	4.08
R143a + R134a	5.16	1.57	12.63	4.55	8.46	2.81	4.09	3.86
Mean	**4.10**	**1.47**	**11.74**	**4.53**	**6.28**	**2.86**	**3.49**	**3.55**
R32 + R125 + R134a	3.72	1.51	13.18	5.33	4.74	2.73	3.70	3.32
R125 + R143a + R134a	3.59	1.21	9.66	3.70	6.60	2.72	2.72	3.42
Mean	**3.65**	**1.36**	**11.61**	**4.52**	**5.76**	**2.72**	**3.26**	**3.37**
	h_m^R				g_m^R			
R32 + R125	3.23	1.32	9.44	4.23	3.83	2.38	3.41	2.97
R32 + R134a	5.44	1.66	12.58	5.04	5.94	2.37	4.49	3.31
R125 + R134a	3.36	1.10	7.01	2.79	5.49	1.82	2.04	2.42
R125 + R143a	4.15	1.20	7.22	3.32	6.87	2.70	3.04	3.65
R143a + R134a	5.38	1.44	10.29	3.97	7.63	2.25	4.08	3.39
Mean	**4.16**	**1.35**	**9.41**	**3.87**	**5.89**	**2.29**	**3.44**	**3.15**
R32 + R125 + R134a	3.62	1.39	10.51	4.45	4.50	2.19	3.63	2.96
R125 + R143a + R134a	3.85	1.13	7.70	3.23	6.37	2.18	2.76	3.08
Mean	**3.75**	**1.26**	**9.26**	**3.84**	**5.53**	**2.18**	**3.24**	**3.02**

5.2. Validation of the EEoS-NN Models Trained on Density and Coexistence Data

The corresponding results for the EEoS-NN models are reported in Tables VII–IX. The performance improvement achieved by the correction

Table V. Accuracy of the SRK Equation for Thermodynamic Quantities Depending on Second Derivatives of Residual Helmholtz Energy in the Three Main Thermodynamic Regions

	AAD (%)							
	sc	l	v	Overall	sc	l	v	Overall
Mixture	$c_{v,m}^R$				$C_{v,m}$			
R32 + R125	48.88	30.22	69.97	46.16	8.33	6.26	6.08	6.58
R32 + R134a	52.39	31.08	73.71	44.93	11.01	7.16	7.00	7.50
R125 + R134a	39.29	41.35	67.51	47.00	5.33	6.74	3.90	5.88
R125 + R143a	40.36	41.95	65.45	47.50	4.94	6.54	3.60	5.47
R143a + R134a	40.69	39.21	71.14	46.61	6.11	6.83	4.67	6.25
Mean	**43.80**	**36.86**	**69.68**	**46.43**	**6.82**	**6.73**	**5.17**	**6.34**
R32 + R125 + R134a	49.85	30.82	71.20	45.73	8.84	6.69	5.73	6.72
R125 + R143a + R134a	40.21	41.39	66.68	47.34	5.12	6.79	3.32	5.64
Mean	**44.55**	**36.19**	**69.18**	**46.53**	**6.80**	**6.74**	**4.65**	**6.18**
	$c_{p,m}^R$				$C_{p,m}$			
R32 + R125	11.01	15.84	31.87	20.02	6.25	8.03	6.15	7.11
R32 + R134a	12.54	17.29	36.45	22.07	8.19	8.71	7.31	8.28
R125 + R134a	10.23	10.61	28.71	14.67	5.67	4.63	4.26	4.70
R125 + R143a	12.14	14.18	27.58	17.11	6.29	6.12	4.02	5.63
R143a + R134a	12.23	14.46	33.21	18.38	7.11	6.29	5.39	6.20
Mean	**11.57**	**14.43**	**31.71**	**18.46**	**6.55**	**6.73**	**5.53**	**6.39**
R32 + R125 + R134a	11.15	14.71	33.80	19.91	6.54	7.34	5.86	6.78
R125 + R143a + R134a	11.39	11.66	29.15	15.87	5.95	5.07	3.67	4.89
Mean	**11.28**	**13.16**	**31.72**	**17.90**	**6.22**	**6.19**	**4.88**	**5.84**
	w_m							
R32 + R125	7.94	23.18	0.57	13.27				
R32 + R134a	10.64	23.73	0.89	16.15				
R125 + R134a	7.49	24.81	0.41	16.66				
R125 + R143a	7.14	25.17	0.61	15.25				
R143a + R134a	8.46	24.39	0.76	16.91				
Mean	**8.08**	**24.27**	**0.65**	**15.64**				
R32 + R125+R134a	8.77	23.67	0.61	14.56				
R125 + R143a + R134a	7.16	25.02	0.47	15.80				
Mean	**7.89**	**24.36**	**0.55**	**15.18**				

through the scale factors is very high; in most cases the deviations are reduced by two orders of magnitude compared to the SRK EoS.

Table VII shows the performances of the EEoS-NN models with respect to properties depending on first derivatives of the residual Helmholtz energy; these results have to be compared with Table IV for the

Table VI. Accuracy of the SRK Equation for VLE Conditions at the Bubble and Dew Points

Mixture	AAD (%)				AAD	
	P^{sat}_{bubble}	P^{sat}_{dew}	ρ^{sl}	ρ^{sv}	$\bar{x}^{sat}_{dew}$	$\bar{y}^{sat}_{bubble}$
R32 + R125	0.86	0.82	7.79	2.28	0.0023	0.0023
R32 + R134a	1.03	0.79	7.37	2.18	0.0034	0.0034
R125 + R134a	0.84	0.72	6.26	1.25	0.0020	0.0020
R125 + R143a	2.99	3.02	7.53	1.44	0.0048	0.0047
R143a + R134a	1.62	1.40	6.61	1.06	0.0029	0.0029
Mean	**1.43**	**1.31**	**7.08**	**1.63**	**0.0031**	**0.0030**
R32 + R125 + R134a	0.86	0.61	6.98	2.20	0.0027	0.0021
R125 + R143a + R134a	2.16	1.75	6.35	0.99	0.0036	0.0033
Mean	**1.50**	**1.17**	**6.67**	**1.60**	**0.0031**	**0.0027**

SRK EoS. The values for the residual compressibility factor Z^R_m in the liquid phase are particularly impressive, since this property is described with very low deviations. The deviations for the other residual properties are absolutely satisfactory, also considering that no information for them was supplied to the regression procedure. Although maintaining an excellent overall performance, it can be observed that the poor performances of the SRK model on the properties u^R_m and s^R_m, involving only temperature derivatives of the a^R_m function, have consequences also on the representation of the same properties obtained by the EEoS-NN model. In general, a limited worsening performance is found when ternary mixtures are considered.

Table VIII shows mean deviations of the proposed models with respect to $c^R_{v,m}$, $c^R_{p,m}$, $C_{v,m}$, $C_{p,m}$, and w_m for binary and ternary mixtures. The description of these second-order properties by the EEoS-NN models has to be regarded as predictive, and consequently the obtained results are rather satisfactory. The residual caloric properties $c^R_{v,m}$ and $c^R_{p,m}$ are homogenously represented with an acceptable accuracy in the three thermodynamic regions; for $C_{v,m}$, $C_{p,m}$, and w_m the best results are found in the vapor region, where the ideal part of each of these properties gives the prevailing contribution to the overall value, allowing for a "dilution" of the deviation for the residual part. In the liquid phase the heat capacities are predicted worse, but in any case the derivations are comparable with the experimental uncertainties for these properties.

VLE data are reproduced in an excellent way as well, as shown in Table IX. The saturated liquid density is represented with a higher accuracy than the saturated vapor density. This is coherent with the results for Z^R_m in the compressed liquid and superheated vapor regions reported in Table VII.

Table VII. Accuracy of the EEoS-NN Models for Thermodynamic Quantities Depending on First Derivatives of Residual Helmholtz Energy; Training on Density and Coexistence Data

	AAD (%)							
	sc	l	v	Overall	sc	l	v	Overall
Mixture	Z_m^R				s_m^R			
R32 + R125	0.122	0.003	0.134	0.066	0.455	0.357	0.839	0.527
R32 + R134a	0.143	0.001	0.070	0.033	0.466	0.170	0.356	0.742
R125 + R134a	0.057	0.001	0.055	0.022	0.264	0.112	0.356	0.191
R125 + R143a	0.036	0.001	0.045	0.019	0.131	0.081	0.377	0.166
R143a + R134a	0.045	0.001	0.055	0.019	0.266	0.177	0.569	0.278
Mean	**0.076**	**0.001**	**0.076**	**0.032**	**0.301**	**0.176**	**0.517**	**0.382**
R32 + R125 + R134a	0.541	0.009	0.467	0.225	1.372	0.612	1.577	1.013
R125 + R143a + R134a	0.308	0.006	0.277	0.127	1.260	0.475	1.506	0.868
Mean	**0.413**	**0.007**	**0.382**	**0.176**	**1.310**	**0.542**	**1.545**	**0.941**
	u_m^R				a_m^R			
R32 + R125	0.308	0.208	0.537	0.330	0.139	0.038	0.117	0.081
R32 + R134a	0.313	0.097	0.470	0.221	0.143	0.019	0.058	0.042
R125 + R134a	0.178	0.067	0.226	0.120	0.061	0.023	0.042	0.033
R125 + R143a	0.090	0.059	0.235	0.109	0.037	0.026	0.032	0.030
R143a + R134a	0.173	0.102	0.354	0.168	0.057	0.022	0.041	0.031
Mean	**0.202**	**0.104**	**0.379**	**0.190**	**0.083**	**0.025**	**0.062**	**0.044**
R32 + R125 + R134a	0.944	0.343	1.010	0.632	0.661	0.096	0.472	0.292
R125 + R143a + R134a	0.895	0.266	0.944	0.545	0.351	0.085	0.245	0.172
Mean	**0.917**	**0.304**	**0.981**	**0.589**	**0.491**	**0.090**	**0.371**	**0.232**
	h_m^R				g_m^R			
R32 + R125	0.252	0.184	0.410	0.268	0.130	0.028	0.121	0.076
R32 + R134a	0.258	0.086	0.358	0.178	0.136	0.015	0.060	0.039
R125 + R134a	0.144	0.059	0.172	0.097	0.059	0.017	0.044	0.029
R125 + R143a	0.075	0.051	0.179	0.088	0.036	0.020	0.035	0.027
R143a + R134a	0.139	0.091	0.268	0.137	0.052	0.017	0.045	0.028
Mean	**0.165**	**0.092**	**0.288**	**0.154**	**0.079**	**0.019**	**0.065**	**0.040**
R32 + R125 + R134a	0.787	0.306	0.804	0.526	0.604	0.072	0.461	0.267
R125 + R143a + R134a	0.757	0.237	0.722	0.449	0.331	0.062	0.242	0.155
Mean	**0.771**	**0.271**	**0.767**	**0.488**	**0.454**	**0.067**	**0.363**	**0.211**

Summarizing, a large improvement of performance was attained moving from the simple SRK equation to the EEoS-NN model. Even though the regression of the scale factor functions was based only on density and VLE data, the obtained equations show good predictions also for thermodynamic properties not involved in the training process.

Table VIII. Accuracy of the EEoS-NN Models for Thermodynamic Quantities Depending on Second Derivatives of Residual Helmholtz Energy; Training on Density and Coexistence Data

	AAD (%)							
	sc	l	v	Overall	sc	l	v	Overall
Mixture	$c_{v,\mathrm{m}}^{\mathrm{R}}$				$C_{v,\mathrm{m}}$			
R32 + R125	9.157	7.582	7.213	7.752	1.469	1.568	0.656	1.262
R32 + R134a	8.406	4.292	7.153	5.492	1.715	1.050	0.684	1.017
R125 + R134a	4.905	2.599	4.029	3.270	0.624	0.422	0.307	0.426
R125 + R143a	2.823	1.083	5.074	2.446	0.362	0.170	0.253	0.231
R143a + R134a	5.316	8.548	5.686	7.466	0.735	1.658	0.405	1.250
Mean	**5.893**	**4.856**	**5.967**	**5.305**	**0.917**	**0.981**	**0.480**	**0.841**
R32 + R125+R134a	7.146	17.563	7.173	12.913	1.254	3.827	0.693	2.508
R125 + R143a + R134a	11.503	9.045	9.178	9.523	1.498	1.373	0.567	1.199
Mean	**9.541**	**13.236**	**8.068**	**11.225**	**1.388**	**2.581**	**0.637**	**1.856**
	$c_{p,\mathrm{m}}^{\mathrm{R}}$				$C_{p,\mathrm{m}}$			
R32 + R125	1.806	1.864	2.955	2.198	0.990	0.870	0.674	0.830
R32 + R134a	2.063	1.053	2.670	1.598	1.286	0.517	0.600	0.618
R125 + R134a	0.881	0.659	1.571	0.900	0.495	0.271	0.337	0.320
R125 + R143a	0.629	0.190	2.025	0.741	0.314	0.078	0.272	0.176
R143a + R134a	0.846	2.671	2.094	2.294	0.489	1.086	0.412	0.853
Mean	**1.182**	**1.308**	**2.324**	**1.552**	**0.667**	**0.571**	**0.477**	**0.562**
R32 + R125 + R134a	3.706	4.486	3.533	4.085	2.530	2.027	0.756	1.720
R125 + R143a + R134a	2.503	1.510	4.050	2.309	1.402	0.632	0.715	0.792
Mean	**3.045**	**2.974**	**3.764**	**3.200**	**1.910**	**1.318**	**0.738**	**1.258**
	w_{m}							
R32 + R125	0.749	0.885	0.055	0.598				
R32 + R134a	0.808	0.625	0.066	0.490				
R125+R134a	0.342	0.181	0.024	0.169				
R125 +R143a	0.176	0.139	0.013	0.116				
R143a + R134a	0.364	0.323	0.027	0.262				
Mean	**0.459**	**0.422**	**0.039**	**0.329**				
R32 + R125 + R134a	1.038	1.988	0.085	1.277				
R125 + R143a + R134a	1.132	0.950	0.066	0.768				
Mean	**1.090**	**1.461**	**0.077**	**1.023**				

5.3. Validation of the EEoS-NN Models Trained on Multiproperty Data

The validation procedure was repeated for the model trained on generated values of the four thermodynamic quantities Z^{R}, c_v^{R}, c_p^{R}, w plus the VLE data. For the sake of brevity the study was carried out for only one mixture, i.e., for the R32 + R134a system.

Table IX. Accuracy of the EEoS-NN Models for VLE Conditions at Bubble and Dew Points; Training on Density and Coexistence Data

Mixture	AAD (%)				AAD	
	P^{sat}_{bubble}	P^{sat}_{dew}	ρ^{sl}	ρ^{sv}	$\bar{x}^{sat}_{dew}$	$\bar{y}^{sat}_{bubble}$
R32 + R125	0.120	0.121	0.042	0.224	0.0001	0.0001
R32 + R134a	0.064	0.068	0.025	0.107	0.0001	0.0001
R125 + R134a	0.077	0.078	0.022	0.110	0.0000	0.0000
R125 + R143a	0.088	0.088	0.020	0.051	0.0000	0.0000
R143a + R134a	0.080	0.083	0.021	0.072	0.0000	0.0000
Mean	**0.084**	**0.086**	**0.026**	**0.111**	**0.0000**	**0.0000**
R32 + R125 + R134a	0.264	0.321	0.181	0.710	0.0006	0.0005
R125 + R143a + R134a	0.177	0.189	0.072	0.668	0.0002	0.0003
Mean	**0.221**	**0.256**	**0.127**	**0.689**	**0.0004**	**0.0004**

Comparing the present results reported in Table X with those obtained for the model trained on density and VLE data, Tables VII and VIII, it can be noted that the performance in the representation of first-order properties is decreased more or less for all of them, but in general not significantly. On the contrary, for the heat capacities an evident improvement is attained, in particular, for the isochoric heat capacity. The representation of the speed of sound is improved as well, but to a lower extent than for the other properties. Therefore, the inclusion of second-order quantities in the training set improves the accuracy of the EEoS-NN model for the same quantities, because information about higher-order derivatives of a^{R}_{m} is supplied to the model.

The validation results for the vapor–liquid coexistence locus, reported in Table XI, are good and show a level of accuracy rather similar to the one obtained for the model trained on density and coexistence data only, Table IX.

A further training case, which involves density, VLE, and speed of sound data in the regression process, was considered. This set of data corresponds to the thermodynamic properties involving first-order derivatives of the residual Helmholtz energy function and the speed of sound, which can be measured with great accuracy. The validation results reported in Tables X and XI show an improvement in the performance on speed of sound compared to the former case, although slightly sacrificing the accuracy on heat capacities. The other properties are reproduced approximately at the same level as before.

Table X. Accuracy of the EEoS-NN Model for the R32 + R134a Mixture for Thermodynamic Quantities Depending on First and Second Derivatives of Residual Helmholtz Energy; Multiproperty Training Cases

Training	Phase	AAD (%)										
		Z_m^R	a_m^R	u_m^R	s_m^R	h_m^R	g_m^R	$c_{v,m}^R$	$c_{p,m}^R$	$C_{v,m}$	$C_{p,m}$	w_m
Z^R, c_v^R, c_p^R, w + VLE	sc	0.263	0.300	0.384	0.689	0.301	0.271	1.954	1.295	0.446	0.963	0.404
	l	0.010	0.029	0.112	0.175	0.099	0.025	0.402	0.258	0.091	0.126	0.393
	v	0.342	0.347	1.007	1.566	0.743	0.335	1.218	0.805	0.130	0.172	0.115
	Overall	0.127	0.144	0.385	0.609	0.296	0.135	0.783	0.513	0.138	0.223	0.318
Z^R, w + VLE	sc	0.349	0.380	0.526	0.676	0.482	0.368	5.612	3.095	1.117	2.318	0.511
	l	0.005	0.037	0.159	0.288	0.140	0.027	8.781	3.060	2.051	1.410	0.138
	v	0.193	0.167	0.675	1.068	0.512	0.171	6.394	2.440	0.564	0.496	0.069
	Overall	0.091	0.107	0.338	0.541	0.276	0.101	7.807	2.893	1.549	1.251	0.157
Z^R + VLE	Overall	0.033	0.042	0.221	0.742	0.178	0.039	5.492	1.598	1.017	0.618	0.490

Table XI. Accuracy of the EEoS-NN Model for the R32 + R134a Mixture for VLE Conditions at Bubble and Dew Points; Multiproperty Training Cases

Training	AAD (%)				AAD	
	P^{sat}_{bubble}	P^{sat}_{dew}	ρ^{sl}	ρ^{sv}	$\bar{x}^{sat}_{dew}$	$\bar{y}^{sat}_{bubble}$
Z^R, c^R_v, c^R_p, w + VLE	0.142	0.155	0.124	0.257	0.0004	0.0004
Z^R, w + VLE	0.171	0.186	0.089	0.412	0.0003	0.0003
Z^R + VLE	0.064	0.068	0.025	0.107	0.0001	0.0001

6. CONCLUSIONS

A new modeling method for developing a dedicated EoS, which was formerly proposed for pure fluids [18], has been extended to mixtures. The method, synthetically indicated as EEoS-NN, recovers the basic framework of the extended corresponding states technique, but a basic equation is assumed instead of a reference fluid. This allows the exclusion of the conformality requirement and of the necessity of an EoS for a reference fluid, because an equation for the target system itself is assumed as a reference. It was demonstrated that a simple equation, such as the SRK cubic EoS applied to a mixture as a one-fluid model with van der Waals mixing rules, is sufficient for such a purpose.

A powerful function approximator in the form of a MLFN was integrated into the model to represent the mixture scale functions. The DEoS of a target mixture is then obtained through a training procedure that determines the individual coefficients of the mixture scale functions through regression on experimental data of thermodynamic properties for the system of interest.

Based on generated data, the performance of the proposed method was verified for some haloalkanes systems. Five binary mixtures and two ternary mixtures were considered, obtaining very promising results.

The study has shown that precise density and VLE mixture data are sufficient to train an EEoS-NN model to excellently represent thermodynamic properties involving the first derivatives of the Helmholtz energy function and to satisfactorily represent those properties involving the second and cross derivatives of a^R_m. The performance of the model on these properties can be improved by including data for such quantities into the training set, according to the requirements that the obtained DEoS has to fulfill.

The satisfactory results obtained in this study with generated data show that the proposed method is an effective modeling technique for the

development of a DEoS for a mixture of interest from multiproperty data. It is an alternative to the presently available most advanced methods.

Having verified such promising performances for the proposed model based on generated data, it is now possible to reliably develop a mixture DEoS in the EEoS-NN format directly from experimental data.

APPENDIX

Calculation of Thermodynamic Properties for a Mixture from an Equation of State in EEoS-NN Format

The equations required for the calculation of the thermodynamic properties of a mixture according to the proposed EEoS-NN format are given here. As previously explained, the subscript m refers to the mixture of interest, while the subscript 0 denotes values calculated from the basic equation for the model, which in the present case is the SRK cubic EoS [19, 20, 22] with the mixing rules of van der Waals for the parameters. The independent variables of the EEoS model and of the basic equation are related by

$$T_0 = T_\mathrm{m}/f_\mathrm{m} \quad \rho_0 = \rho_\mathrm{m} h_\mathrm{m} \tag{A1, A2}$$

while the mole fraction array $\bar{z}$ is the same. The main thermodynamic properties considered in this work are obtained as:

Compressibility factor:
$$Z_\mathrm{m}^\mathrm{R} \equiv P_\mathrm{m}/\rho_\mathrm{m} R T_\mathrm{m} - 1 = F_\rho\, u_0^\mathrm{R} + \left(1 + H_\rho\right) Z_0^\mathrm{R} \tag{A3}$$

Helmholtz energy:
$$a_\mathrm{m}^\mathrm{R} = A_\mathrm{m}^\mathrm{R}/RT_\mathrm{m} = a_0^\mathrm{R} \tag{A4}$$

Internal energy:
$$u_\mathrm{m}^\mathrm{R} = U_\mathrm{m}^\mathrm{R}/RT_\mathrm{m} = (1 - F_T)\, u_0^\mathrm{R} - H_T\, Z_0^\mathrm{R} \tag{A5}$$

Enthalpy:
$$h_\mathrm{m}^\mathrm{R} = H_\mathrm{m}^\mathrm{R}/RT_\mathrm{m} = h_0^\mathrm{R} + \left(F_\rho - F_T\right) u_0^\mathrm{R} + \left(H_\rho - H_T\right) Z_0^\mathrm{R} \tag{A6}$$

Gibbs energy:
$$g_\mathrm{m}^\mathrm{R} = G_\mathrm{m}^\mathrm{R}/RT_\mathrm{m} = g_0^\mathrm{R} + F_\rho\, u_0^\mathrm{R} + H_\rho\, Z_0^\mathrm{R} \tag{A7}$$

Entropy:
$$s_\mathrm{m}^\mathrm{R} = S_\mathrm{m}^\mathrm{R}/R = s_0^\mathrm{R} - F_T\, u_0^\mathrm{R} - H_T\, Z_0^\mathrm{R} \tag{A8}$$

Isochoric heat capacity:
$$c_{v,\mathrm{m}}^\mathrm{R} = C_{v,\mathrm{m}}^\mathrm{R}/R = -T_\mathrm{m}^2 \left(\frac{\partial^2 a_\mathrm{m}^\mathrm{R}}{\partial T_\mathrm{m}^2}\right)_{\rho_\mathrm{m}, \bar{z}} + 2u_\mathrm{m}^\mathrm{R} \tag{A9}$$

Isobaric heat capacity:
$$c^{\mathrm{R}}_{p,\mathrm{m}} = C^{\mathrm{R}}_{p,\mathrm{m}} \Big/ R = c^{\mathrm{R}}_{v,\mathrm{m}} + \frac{\left[1 + Z^{\mathrm{R}}_{\mathrm{m}} + \rho_{\mathrm{m}} T_{\mathrm{m}} \left(\frac{\partial^2 a^{\mathrm{R}}_{\mathrm{m}}}{\partial \rho_{\mathrm{m}} \partial T_{\mathrm{m}}}\right)_{\bar{z}}\right]^2}{1 + 2Z^{\mathrm{R}}_{\mathrm{m}} + \rho^2_{\mathrm{m}} \left(\frac{\partial^2 a^{\mathrm{R}}_{\mathrm{m}}}{\partial \rho^2_{\mathrm{m}}}\right)_{T_{\mathrm{m}},\bar{z}}} - 1 \tag{A10}$$

Speed of sound:
$$w_{\mathrm{m}} = \sqrt{\frac{R T_{\mathrm{m}}}{M_{\mathrm{m}}} \frac{C_{p,\mathrm{m}}}{C_{v,\mathrm{m}}} \left[1 + 2Z^{\mathrm{R}}_{\mathrm{m}} + \rho^2_{\mathrm{m}} \left(\frac{\partial^2 a^{\mathrm{R}}_{\mathrm{m}}}{\partial \rho^2_{\mathrm{m}}}\right)_{T_{\mathrm{m}},\bar{z}}\right]} \tag{A11}$$

Partial molar fugacity coefficient:
$$\ln \hat{\varphi}_i = \left[\frac{\partial\,(n \ln \varphi_{\mathrm{m}})}{\partial n_i}\right]_{P_{\mathrm{m}},T_{\mathrm{m}},n_{j\neq i}} = \ln \hat{\varphi}_{0,i} - \ln\left[1 + u^{\mathrm{R}}_0 F_\rho + Z^{\mathrm{R}}_0 \left(1 + H_\rho\right)\right] + \ln\left(1 + Z^{\mathrm{R}}_0\right) + u^{\mathrm{R}}_0 \left(F_{n_i} + F_\rho\right) + Z^{\mathrm{R}}_0 \left(H_{n_i} + H_\rho\right) \tag{A12}$$

The second derivatives in Eqs. (A9)–(A11) are calculated with the following equations:
$$T^2_{\mathrm{m}} \left(\frac{\partial^2 a^{\mathrm{R}}_{\mathrm{m}}}{\partial T^2_{\mathrm{m}}}\right)_{\rho_{\mathrm{m}},\bar{z}} = T^2_0 \left(\frac{\partial^2 a^{\mathrm{R}}_0}{\partial T^2_0}\right)_{\rho_0,\bar{z}} (1 - F_T)^2 + 2\rho_0 T_0 \left(\frac{\partial^2 a^{\mathrm{R}}_0}{\partial \rho_0 \partial T_0}\right)_{\bar{z}} H_T (1 - F_T) + Z^{\mathrm{R}}_0 H_{TT} - u^{\mathrm{R}}_0 \left(2F^2_T - 2F_T - F_{TT}\right) + \rho^2_0 \left(\frac{\partial^2 a^{\mathrm{R}}_0}{\partial \rho^2_0}\right)_{T_0,\bar{z}} H^2_T \tag{A13}$$

$$\rho^2_{\mathrm{m}} \left(\frac{\partial^2 a^{\mathrm{R}}_{\mathrm{m}}}{\partial \rho^2_{\mathrm{m}}}\right)_{T_{\mathrm{m}},\bar{z}} = T^2_0 \left(\frac{\partial^2 a^{\mathrm{R}}_0}{\partial T^2_0}\right)_{\rho_0,\bar{z}} F^2_\rho - 2\rho_0 T_0 \left(\frac{\partial^2 a^{\mathrm{R}}_0}{\partial \rho_0 \partial T_0}\right)_{\bar{z}} F_\rho \left(1 + H_\rho\right) + + Z^{\mathrm{R}}_0 \left(2H_\rho + H_{\rho\rho}\right) - u^{\mathrm{R}}_0 \left(2F^2_\rho - F_{\rho\rho}\right) + \rho^2_0 \left(\frac{\partial^2 a^{\mathrm{R}}_0}{\partial \rho^2_0}\right)_{T_0,\bar{z}} \left(1 + H_\rho\right)^2 \tag{A14}$$

$$\rho_{\mathrm{m}} T_{\mathrm{m}} \left(\frac{\partial^2 a_{\mathrm{m}}^{\mathrm{R}}}{\partial \rho_{\mathrm{m}} \partial T_{\mathrm{m}}} \right)_{\bar{z}} = T_0^2 \left(\frac{\partial^2 a_0^{\mathrm{R}}}{\partial T_0^2} \right)_{\rho_0, \bar{z}} F_\rho \left(F_T - 1 \right) + \rho_0 T_0 \left(\frac{\partial^2 a_0^{\mathrm{R}}}{\partial \rho_0 \partial T_0} \right)_{\bar{z}} \left[\left(1 + H_\rho \right) \left(1 - F_T \right) - F_\rho H_T \right] + Z_0^{\mathrm{R}} \left(H_T + H_{\rho T} \right) - u_0^{\mathrm{R}} \left(2 F_T F_\rho - F_\rho - F_{\rho T} \right) + \rho_0^2 \left(\frac{\partial^2 a_0^{\mathrm{R}}}{\partial \rho_0^2} \right)_{T_0, \bar{z}} H_T \left(1 + H_\rho \right) \tag{A15}$$

The logarithmic derivatives of the scale factor functions are defined as

$$F_\rho \equiv \frac{\rho_{\mathrm{m}}}{f_{\mathrm{m}}} \left(\frac{\partial f_{\mathrm{m}}}{\partial \rho_{\mathrm{m}}} \right)_{T_{\mathrm{m}}, \bar{z}} \qquad H_\rho \equiv \frac{\rho_{\mathrm{m}}}{h_{\mathrm{m}}} \left(\frac{\partial h_{\mathrm{m}}}{\partial \rho_{\mathrm{m}}} \right)_{T_{\mathrm{m}}, \bar{z}} \tag{A16, A17}$$

$$F_T \equiv \frac{T_{\mathrm{m}}}{f_{\mathrm{m}}} \left(\frac{\partial f_{\mathrm{m}}}{\partial T_{\mathrm{m}}} \right)_{\rho_{\mathrm{m}}, \bar{z}} \qquad H_T \equiv \frac{T_{\mathrm{m}}}{h_{\mathrm{m}}} \left(\frac{\partial h_{\mathrm{m}}}{\partial T_{\mathrm{m}}} \right)_{\rho_{\mathrm{m}}, \bar{z}} \tag{A18, A19}$$

$$F_{\rho\rho} \equiv \frac{\rho_{\mathrm{m}}^2}{f_{\mathrm{m}}} \left(\frac{\partial^2 f_{\mathrm{m}}}{\partial \rho_{\mathrm{m}}^2} \right)_{T_{\mathrm{m}}, \bar{z}} \qquad H_{\rho\rho} \equiv \frac{\rho_{\mathrm{m}}^2}{h_{\mathrm{m}}} \left(\frac{\partial^2 h_{\mathrm{m}}}{\partial \rho_{\mathrm{m}}^2} \right)_{T_{\mathrm{m}}, \bar{z}} \tag{A20, A21}$$

$$F_{TT} \equiv \frac{T_{\mathrm{m}}^2}{f_{\mathrm{m}}} \left(\frac{\partial^2 f_{\mathrm{m}}}{\partial T_{\mathrm{m}}^2} \right)_{\rho_{\mathrm{m}}, \bar{z}} \qquad H_{TT} \equiv \frac{T_{\mathrm{m}}^2}{h_{\mathrm{m}}} \left(\frac{\partial^2 h_{\mathrm{m}}}{\partial T_{\mathrm{m}}^2} \right)_{\rho_{\mathrm{m}}, \bar{z}} \tag{A22, A23}$$

$$F_{\rho T} \equiv \frac{\rho_{\mathrm{m}} T_{\mathrm{m}}}{f_{\mathrm{m}}} \left(\frac{\partial^2 f_{\mathrm{m}}}{\partial \rho_{\mathrm{m}} \partial T_{\mathrm{m}}} \right)_{\bar{z}} \qquad H_{\rho T} \equiv \frac{\rho_{\mathrm{m}} T_{\mathrm{m}}}{h_{\mathrm{m}}} \left(\frac{\partial^2 h_{\mathrm{m}}}{\partial \rho_{\mathrm{m}} \partial T_{\mathrm{m}}} \right)_{\bar{z}} \tag{A24, A25}$$

$$F_{n_i} = \left(\frac{\partial f_{\mathrm{m}}}{\partial n_i} \right)_{T_{\mathrm{m}}, \rho_{\mathrm{m}}, n_{j \neq i}} \left(\frac{n_i}{f_{\mathrm{m}}} \right) = \frac{1}{f_{\mathrm{m}}} \left\{ \left(\frac{\partial f_{\mathrm{m}}}{\partial z_i} \right)_{T_{\mathrm{m}}, \rho_{\mathrm{m}}, z_{j \neq i}} - \sum_{k=1}^{C-1} \left[z_k \left(\frac{\partial f_{\mathrm{m}}}{\partial z_k} \right)_{T_{\mathrm{m}}, \rho_{\mathrm{m}}, z_{j \neq k}} \right] \right\} \tag{A26}$$

$$H_{n_i} = \left(\frac{\partial h_{\mathrm{m}}}{\partial n_i} \right)_{T_{\mathrm{m}}, \rho_{\mathrm{m}}, n_{j \neq i}} \left(\frac{n_i}{h_{\mathrm{m}}} \right) = \frac{1}{h_{\mathrm{m}}} \left\{ \left(\frac{\partial h_{\mathrm{m}}}{\partial z_i} \right)_{T_{\mathrm{m}}, \rho_{\mathrm{m}}, z_{j \neq i}} - \sum_{k=1}^{C-1} \left[z_k \left(\frac{\partial h_{\mathrm{m}}}{\partial z_k} \right)_{T_{\mathrm{m}}, \rho_{\mathrm{m}}, z_{j \neq k}} \right] \right\} \tag{A27}$$

If the SRK cubic equation is selected as the basic equation for the EEoS model, the quantities in Eqs. (A3)–(A15) are calculated with the following expressions:

$$a_0^{\mathrm{R}} - \ln\left[1+(c-b)\,\rho_0\right] - \frac{a_{\mathrm{SRK}}}{RT_0 b}\ln\left[\frac{1+(c+b)\,\rho_0}{1+c\rho_0}\right] \tag{A28}$$

$$Z_0^{\mathrm{R}} = -\frac{(c-b)\,\rho_0}{1+(c-b)\;\rho_0} - \frac{a_{\mathrm{SRK}}}{RT_0 b}\left[\frac{(c+b)\;\rho_0}{1+(c+b)\;\rho_0} - \frac{c\,\rho_0}{1+c\,\rho_0}\right] \tag{A29}$$

$$u_0^{\mathrm{R}} = \frac{1}{Rb}\left(\frac{\partial a_{\mathrm{SRK}}}{\partial T_0} - \frac{a_{\mathrm{SRK}}}{T_0}\right)\ln\left[\frac{1+(c+b)\;\rho_0}{1+c\,\rho_0}\right] \tag{A30}$$

$$h_0^{\mathrm{R}} = u_0^{\mathrm{R}} + Z_0^{\mathrm{R}} \tag{A31}$$

$$g_0^{\mathrm{R}} = a_0^{\mathrm{R}} + Z_0^{\mathrm{R}} \tag{A32}$$

$$s_0^{\mathrm{R}} = u_0^{\mathrm{R}} - a_0^{\mathrm{R}} \tag{A33}$$

$$\left(\frac{\partial^2 a_0^{\mathrm{R}}}{\partial T_0^2}\right)_{\rho_0} = -\frac{1}{RbT_0}\left(\frac{\partial^2 a_{\mathrm{SRK}}}{\partial T_0^2} - \frac{2}{T_0}\frac{\partial a_{\mathrm{SRK}}}{\partial T_0} + \frac{2a_{\mathrm{SRK}}}{T_0^2}\right)\ln\left[\frac{1+(c+b)\;\rho_0}{1+c\,\rho_0}\right] \tag{A34}$$

$$\left(\frac{\partial^2 a_0^{\mathrm{R}}}{\partial \rho_0^2}\right)_{T_0} = \left[\frac{(c-b)}{1+(c-b)\;\rho_0}\right]^2 + \frac{a_{\mathrm{SRK}}}{RT_0 b}\left\{\left[\frac{(c+b)}{1+(c+b)\,\rho_0}\right]^2 - \left(\frac{c}{1+c\rho_0}\right)^2\right\} \tag{A35}$$

$$\left(\frac{\partial^2 a_0^{\mathrm{R}}}{\partial \rho_0\,\partial T_0}\right) = -\frac{1}{RbT_0}\left(\frac{\partial a_{\mathrm{SRK}}}{\partial T_0} - \frac{a_{\mathrm{SRK}}}{T_0}\right)\left[\frac{(c+b)}{1+(c+b)\;\rho_0} - \frac{c}{1+c\,\rho_0}\right] \tag{A36}$$

$$\begin{aligned}\ln\hat{\varphi}_{0,i} = {} & -\ln\left\{\left(1+Z_0^{\mathrm{R}}\right)\left[1+(c-b)\,\rho_0\right]\right\} \\ & -\frac{a_{\mathrm{SRK}}}{RT_0 b}\left(1+\frac{\bar{a}_{\mathrm{SRK},i}}{a_{\mathrm{SRK}}}-\frac{\bar{b}_i}{b}\right)\quad \ln\left[\frac{1+(c+b)\,\rho_0}{1+c\rho_0}\right] \\ & -\frac{\left(\bar{c}_i-\bar{b}_i\right)\rho_0}{1+(c-b)\,\rho_0} - \frac{a_{\mathrm{SRK}}\rho_0}{RT_0 b}\left[\frac{\bar{c}_i+\bar{b}_i}{1+(c+b)\,\rho_0} - \frac{\bar{c}_i}{1+c\rho_0}\right]\end{aligned} \tag{A37}$$

with

$$\bar{a}_{\mathrm{SRK},i} \equiv \left[\frac{\partial\left(n a_{\mathrm{SRK}}\right)}{\partial n_i}\right]_{T_0,\rho_0,n_{j\neq i}} \tag{A38}$$

$$\bar{b}_i \equiv \left[\frac{\partial\left(nb\right)}{\partial n_i}\right]_{T_0,\rho_0,n_{j\neq i}} = b_i \tag{A39}$$

$$\bar{c}_i \equiv \left[\frac{\partial (nc)}{\partial n_i}\right]_{T_0,\rho_0,n_{j\neq i}} = c_i \tag{A40}$$

In the present work the scale factors are obtained in the form of a multilayer feedforward neural network. The equations for the calculation of the scale factors and their derivatives are reported in the following. The correspondence of the physical variables of the system with the variables of the neural model is given by

Binary mixtures: $V_1 = T_\mathrm{m} \quad V_2 = \rho_\mathrm{m} \quad V_3 = z_1$ (A41, A42, A43)

Ternary mixtures: $V_1 = T_\mathrm{m} \quad V_2 = \rho_\mathrm{m} \quad V_3 = z_1 \quad V_4 = z_2$ (A44, A45, A46, A47)

All mixtures: $W_1 = f_\mathrm{m} \quad W_2 = h_\mathrm{m}$ (A48, A49)

Neural network inputs

$$U_i = u_i \left(V_i - V_{i,\min}\right) + A_{\min} \text{ with } u_i = \frac{A_{\max} - A_{\min}}{V_{i,\max} - V_{i,\min}} \quad \text{for } 1 \leqslant i \leqslant I-1 \tag{A50, A51}$$

$$U_I = \mathrm{Bias1} \tag{A52}$$

Hidden layer inputs and outputs

$$G_j = \sum_{i=1}^{I} w_{ij} U_i \qquad 1 \leqslant j \leqslant J \tag{A53}$$

$$H_j = g\left(\sum_{i=1}^{I} w_{ij} U_i\right) \quad 1 \leqslant j \leqslant J \tag{A54}$$

$$H_{J+1} = \mathrm{Bias2} \tag{A55}$$

Output layer inputs and outputs

$$R_k = \sum_{j=1}^{J+1} w_{jk} H_j \quad 1 \leqslant k \leqslant K \tag{A56}$$

$$S_k = g\,(R_k) \qquad 1 \leqslant k \leqslant K \tag{A57}$$

Physical variable outputs

$$W_k = \frac{S_k - A_{\min}}{s_k} + W_{k,\min} \quad \text{with } s_k = \frac{A_{\max} - A_{\min}}{W_{k,\max} - W_{k,\min}} \quad \text{for } 1 \leqslant k \leqslant K \tag{A.58, A.59}$$

Output derivatives

$$\frac{\partial W_k}{\partial V_m} = \frac{u_m}{s_k} g'(R_k) \sum_{j=1}^{J} w_{mj} w_{jk} g'(G_j) \quad 1 \leqslant m \leqslant I-1, \quad 1 \leqslant k \leqslant K \tag{A.60}$$

$$\frac{\partial^2 W_k}{\partial V_m \partial V_n} = \frac{u_m u_n}{s_k} g''(R_k) \left[\sum_{j=1}^{J} w_{mj} w_{jk} g'(G_j)\right] \left[\sum_{j=1}^{J} w_{nj} w_{jk} g'(G_j)\right] + \\ + g'(R_k) \left[\sum_{j=1}^{J} w_{mj} w_{nj} w_{jk} g''(G_j)\right] \quad 1 \leqslant m, n \leqslant I-1, \quad 1 \leqslant k \leqslant K \tag{A.61}$$

where

$$g(x) = \frac{1}{\pi} \arctan(\gamma x) + \frac{1}{2} \tag{A.62}$$

$$g'(x) = \frac{d\,g(x)}{d\,x} = \frac{\gamma}{\pi \left[1 + (\gamma x)^2\right]} \tag{A.63}$$

$$g''(x) = \frac{d^2 g(x)}{d\,x^2} = \frac{-2\gamma^3 x}{\pi \left[1 + (\gamma x)^2\right]^2} \tag{A.64}$$

REFERENCES

1. R. Tillner-Roth, *Die Thermodynamischen Eigenschaften von R152a, R134a und Ihren Gemischen*, DKV Forschungsberichte, Nr. 41 (Deutsches Kälte- und Klimatechnischer Verein (DKV), Stuttgart, 1993).
2. R. Tillner-Roth, *Fundamental Equations of State* (Shaker Verlag, Aachen, 1998).
3. E. W. Lemmon and R. T Jacobsen, in *Thermodynamic Properties of Mixtures of Refrigerants R-32, R-125, R-134a and R-152a. Proc. IEA Annex 18*, IEA, Toronto, Canada (1996).
4. R. Tillner-Roth and D. G. Friend, *J. Phys. Chem. Ref. Data* **27**:63 (1998).
5. R. Tillner-Roth, J. Li, A. Yokozeki, H. Sato, and K. Watanabe, *Thermodynamic Properties of Pure and Blended Hydrofluorocarbon (HFC) Refrigerants* (Japan Society of Refrigerating and Air Conditioning Engineers, Tokyo, 1998).
6. E. W. Lemmon and R. Tillner-Roth, *Fluid Phase Equilib*. **165**:1 (1999).
7. E. W. Lemmon and R. T Jacobsen, *Int. J. Thermophys*. **20**:825 (1999).
8. J. W. Leach, P. S. Chappelear, and T. W. Leland, *AIChE J.* **14**:568 (1968).
9. T. W. Leland and P. S. Chappelear, *Ind. Eng. Chem*. **60**:15 (1968).
10. J. Mollerup, *Fluid Phase Equilib*. **4**:11 (1980).

11. J. F. Ely, *Adv. Cryog. Eng*. **35**:1511 (1990).
12. M. L. Huber and J. F. Ely, *Int. J. Refrig*. **17**:18 (1994).
13. J. F. Ely and I. M. Marrucho, in *Equations of State for Fluids and Fluid Mixtures. Part I*, J. V. Sengers, R. F. Kayser, C. J. Peters, and H. J. White Jr., eds. (Elsevier, Amsterdam, 2000), pp. 289–320.
14. W. P. Clarke, R. T. Jacobsen, E. W. Lemmon, S. G. Penoncello, and S. W. Beyerlein, *Int. J Thermophys.* **15**:1289 (1994).
15. A. Nowarski and D. G. Friend, *Int. J. Thermophys.* **19**:1133 (1998).
16. L. Piazza, G. Scalabrin, P. Marchi, and D. Richon, *Int. J. Refrig*. **29**:1182 (2006).
17. G. Scalabrin, P. Marchi, L. Bettio, and D. Richon, *Int. J. Refrig*. **29**:1195 (2006).
18. G. Scalabrin, L. Bettio, P. Marchi, L. Piazza, and D. Richon, *Int. J. Thermophys*. (in press).
19. O. Redlich and J. N. S. Kwong, *Chem. Rev*. **44**:233 (1949).
20. G. Soave, *Chem. Eng. Sci*. **27**:1197 (1972).
21. V. Kůrková, *Neural Networks* **5**:501 (1992).
22. A. Péneloux, E. Rauzy, and R. Fréze, *Fluid Phase Equilib*. **8**:7 (1982).
23. R. Span, *Multiparameter Equations of State* (Springer Verlag, Berlin, 2000).
24. G. Scalabrin, L. Piazza, and G. Cristofoli, *Int. J. Thermophys*. **23**:57 (2002).
25. G. Scalabrin, L. Piazza, and D. Richon, *Fluid Phase Equilib.* **199**:33 (2002).
26. G. Scalabrin, G. Cristofoli, and D. Richon, *Fluid Phase Equilib*. **199**:265 (2002).
27. G. Scalabrin, G. Cristofoli, and D. Richon, *Fluid Phase Equilib*. **199**:281 (2002).
28. G. Scalabrin, P. Marchi, P. Stringari, and D. Richon, *Fluid Phase Equilib.* **242**:72 (2006).
29. G. Scalabrin, P. Marchi, P. Stringari, and D. Richon, *Fluid Phase Equilib.* **242**:79 (2006).
30. R. Tillner-Roth and A. Yokozeki, *J. Phys. Chem. Ref. Data* **26**:1273 (1997).
31. S. L. Outcalt and M. O. McLinden, *Int. J. Thermophys*. **16**:79 (1995).
32. R. Tillner-Roth and H. D. Baehr, *J. Phys. Chem. Ref. Data* **23**:657 (1994).
33. S. L. Outcalt and M. O. McLinden, *Int. J. Thermophys*. **18**:1445 (1997).
34. D. E. Rumelhart and J. L. McClelland, *Parallel Distributed Processing: Exploration in the Microstructure of Cognition* (MIT Press, Cambridge, Massachusetts, 1986).